

Supporting Information:

The Role of Charge-Matching in Nanoporous Materials Formation

Alessia Centi,[†] Joseph R. H. Manning,[‡] Vibha Srivastava,[‡] Sandra van Meurs,[¶]
Siddharth V. Patwardhan,^{*,‡} and Miguel Jorge^{*,†}

[†]*Department of Chemical and Process Engineering, University of Strathclyde, 75 Montrose
Street, Glasgow G1 1XJ*

[‡]*Department of Chemical and Biological Engineering, University of Sheffield, Mappin
Street, Sheffield S1 3JD*

[¶]*Department of Chemistry, University of Sheffield, Brook Hill, Sheffield S3 7HF, United
Kingdom*

E-mail: s.patwardhan@sheffield.ac.uk; miguel.jorge@strath.ac.uk

1 Experimental details

DDA titration pH titration tests on DDA were conducted using a Metrohm 902 Titrando system and Tiamo 2.5 software using the mono endpoint titration (MET) command. Using this, HCl at a concentration of 1 M was added at a constant rate (typically 50 $\mu\text{l}/\text{min}$) during which time the pH was recorded. To determine titration endpoints and hence species pK_a , $\frac{d^2\text{pH}}{dt^2}$ was numerically calculated in OriginPro 2017 using a Savitsky-Gorlay smoothing algorithm (the time derivative was used instead of the volume derivative to increase precision; as $\frac{dV}{dt}$ is constant, this does not affect determination of the inflection points). Inflection points

indicating the titration endpoint were then found by identifying the characteristic point on the second differential curve. From here, the pKa could be calculated as the pH after dosing half of the required acid, as exemplified in Figure 1-a in the main body.

HMS synthesis method Hexagonal mesoporous silica was synthesised according to the procedure first described by Tanev and Pinnavaia¹. Dodecylamine (933 mg, 5 mmol) was dissolved in a mixture of ethanol (10.6 ml, 182 mmol) and water (10.6 ml, 589 mmol) under vigorous stirring at ambient temperature in a 180 ml polypropylene tub. TEOS (4.43 ml, 20 mmol) was then added in a single aliquot, and the tube sealed and left to age under stirring for 18 hours. After this time, the resultant coagulum was decanted into 50 ml centrifuge tubes and spun at 5000 g for 15 minutes three times, washing with water between each spin. After the final spin, the white slurry was scraped into a watch glass for air drying.

Activation of the HMS was performed by calcination at 550 °C in a muffle furnace for 12 hours, after which nitrogen adsorption analysis was performed to confirm that mesoporosity was incorporated successfully. The results of the BET analysis are shown in figure S1

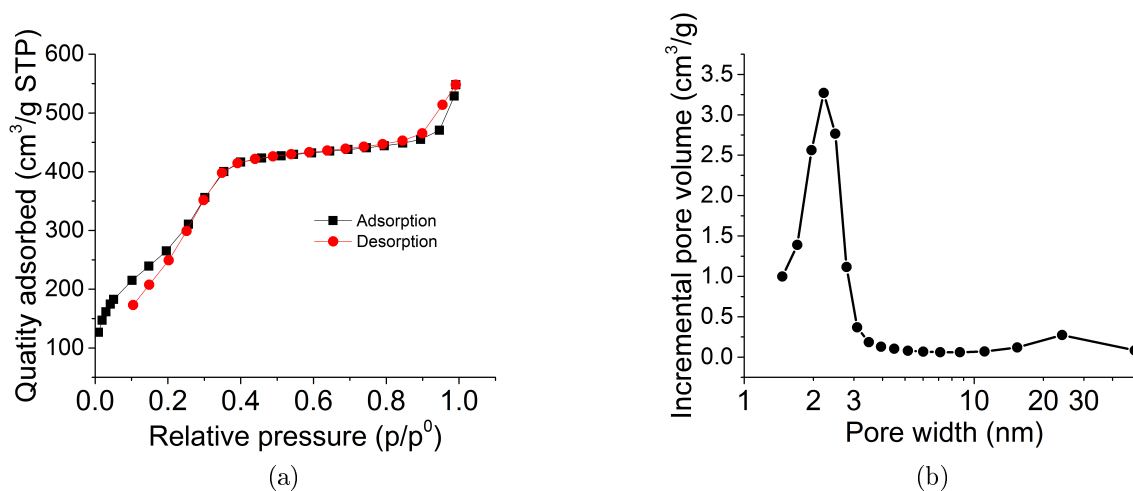


Figure S1: Nitrogen adsorption data for HMS produced in this study: (a) experimental nitrogen isotherm at 77 K showing adsorption (black) and desorption (red), and (b) BJH pore-size distribution, showing a peak at 2.2 nm in accordance with reference¹

Preparation of test DDA solutions for NMR analysis To test a range of solution environments for the DDA molecule and measure their relative NMR spectra compared to the reaction mixture, DDA solutions were made up spiked with HCl or NaCl. Further, a solution with low DDA concentration was made up to replicate the final concentration in the supernatant after HMS precipitation. Table S1 shows the compositions of the solutions used for direct NMR and pH analysis.

Table S1: Composition of various HMS reaction mixture mimics for NMR analysis

Component	Original reaction mixture ^a	DDA starting solution	Low concentration	NaCl doped	Post-hydrolysis solvent	20 % mol protonated ^b	90 % mol protonated ^b	99 % mol protonated ^b
DDA mg (mmol)	933.1 (5.03)	49.6 (0.268)	25.0 (0.135)	164.8 (0.889)	24.8 (0.135)	49.5 (0.267)	164.7 (0.889)	163.5 (0.882)
NaCl mg (mmol)	-	-	-	10.4 (0.179)	-	-	-	-
HCl ml ^c (mmol)	-	-	-	-	-	0.054	0.800	0.890
H ₂ O ml (mmol)	10.6 (589)	0.533 (29.6)	1.75 (97.2)	1.75 (97.2)	1.635 (90.8)	0.479 (29.6) ^d	0.955 (97.5) ^d	0.865 (97.5) ^d
EtOH ml (mmol)	10.6 (182)	0.531 (9.09)	1.75 (29.97)	1.75 (29.97)	2.515 (43.1)	0.531 (9.09)	1.75 (29.97)	1.75 (29.97)

^a Containing 4.43 ml TEOS (20 mmol)

^b as determined by the Henderson-Hasselbalch equation;

^c volume of a 1M aqueous HCl solution

^d including H₂O added with HCl

NMR investigation of HMS deshielding under different conditions Reaction supernatants and test solutions were loaded directly into standard 5 mm NMR tubes which were subsequently fitted with coaxial inserts containing 1 % w/w 4,4-dimethyl-4-silapentane-1-sulfonic acid (DSS) in D₂O to provide a deuterium lock and quantitation reference. NMR spectra were acquired using a Bruker AVANCE III HD spectrometer operating at 500.13 MHz, using a 30 degree flip angle for 16 transients, 10 kHz spectral window, 3.3 s acquisition time (64k points) plus 1 second relaxation delay.

Once collected, NMR shifts were normalised against the DSS trimethylsilyl peak. DDA concentration and chemical environment were analysed through the peak at $\delta \approx 2.78$ ppm, corresponding to the protons on the carbon closest to the amine functionality, referred to as C1 protons (the protons on the amine functionality were impossible to analyse due to their

high exchange frequency with water)².

Through the NMR experiments, neither concentration nor ionic strength were found to have a large effect on the DDA peak shifting, indicating that these variables could not be responsible for the observed shifting from $\delta = 2.78$ ppm to $\delta = 2.85$ ppm. The effect of TEOS hydrolysis on solvent environment was then investigated by changing the relative volumes of ethanol and water in the reaction mixture to correspond with complete hydrolysis and condensation of the TEOS (corresponding to molar concentrations of 0.04 DDA: 27.6 H₂O: 13.09 EtOH). This showed a larger effect, with the observed peak shifting to $\delta = 2.83$ ppm, although significantly this was still unable to replicate the peak shifting associated with the chemical reaction.

Despite this, acidification of the reaction mixture to 20 %, 90 %, and 99 % molar protonation was found to have a significant effect on DDA peak deshielding, with the peaks moving to 2.85, 3.12, and 3.14 ppm, respectively. This more than accounted for the shift in the C1 signal measured in the reaction supernatant, therefore it was concluded that a significant amount of protonation had occurred during the addition of TEOS. NMR spectra for the samples in different chemical environments is shown in Figure S2.

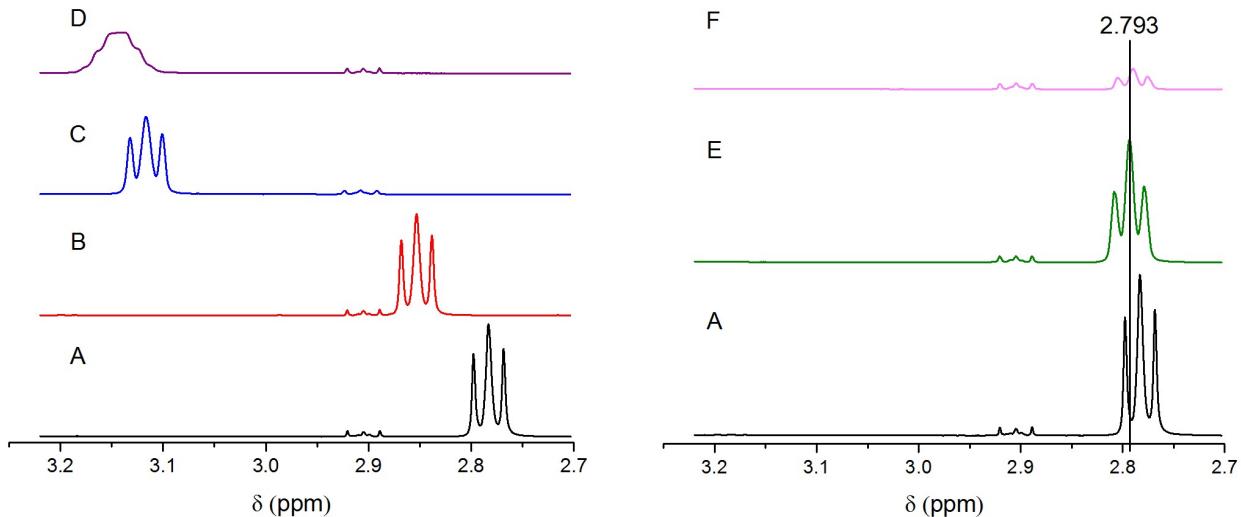


Figure S2: Comparison of NMR spectra taken for the different DDA solutions prepared in this study: (A) DDA starting solution, (B) NaCl doped, (C) Low concentration, (D) Post-hydrolysis solvent, (E) 20 % protonated, (F) 90 % protonated, (G) 99 % protonated. Vertical line represents major peak from reaction mixture at $\delta = 2.85$ ppm

2 Atomistic simulations

Water molecules were modelled using the SPC/E potential³, while the OPLS all-atom force field^{4,5} was used for surfactants and counter-ions. Figure S3 provides a representation of the two types of surfactant (neutral and cationic) considered. Label Hn represents hydrogen atoms belonging to amino groups, with N indicating a nitrogen and Cn a carbon bonded to it. The hydrogens on Cn atoms are referred as Hcn while those on carbons C and C3 in the hydrocarbon chain are called Hc. When the amine heads are charged, the hydrogen atoms in the amino groups take the name Hnc while the nitrogens are indicated by Nc and the carbons bonded to them by Cnc.

Parameters used for silica monomers and dimers were taken from the work of Jorge et al.⁶; a representation of all the inorganic species considered is provided in Figure S4. The nomenclature for silicates is as follows: SiN and SiI are used for neutral and anionic silicons

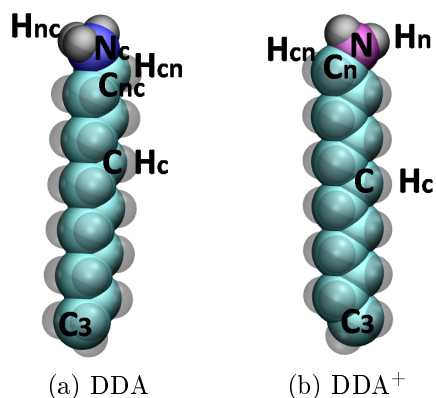


Figure S3: All-atom representation of the dodecylamine surfactants in different charge states: neutral DDA surfactants (a) predominantly exist at high pH (> 12), while at pH lower than 8 only charged DDA⁺ (b) are found. Neutral nitrogens, purple; charged nitrogens, blue; carbons, teal and hydrogens, gray.

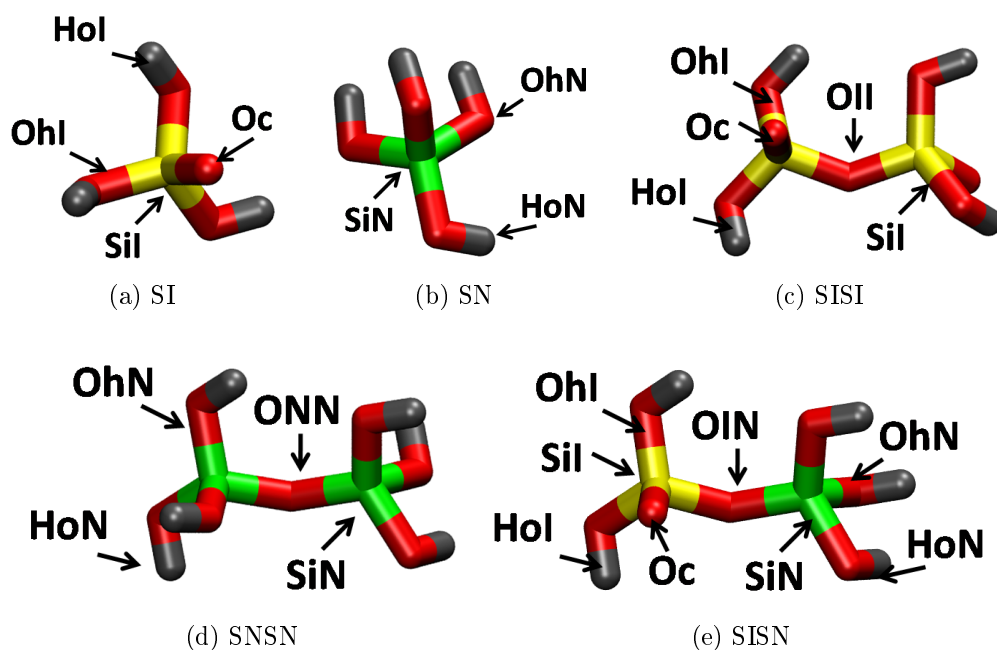


Figure S4: All-atom representations of the different silicate species: SI, anionic monomer; SN, neutral monomer; SISI, dimer with two charges; SNSN, neutral dimer and SISN, dimer with one charge. Neutral silicons, green; charged silicons, yellow; oxygens, red and hydrogens, gray.

respectively, OhN and HoN for oxygen and hydrogen atoms belonging to hydroxyl groups in neutral species, while OhI and HoI are used for the corresponding atoms of hydroxyl groups when these are part of anionic species, Oc is a charged oxygen and finally OII, ONN, and OIN represent oxygen atoms linking, respectively, two anionic silicons, two neutral silicons, or one anionic and one neutral silicon.

Tables S2- S5 contain all force field parameters used for atomistic simulations. The potential energy function is represented as the sum of angle bending, dihedral torsion, Lennard-Jones interactions and Coulomb electrostatic terms. Non-bonded interactions are calculated only for atoms that are separated by three or more bonds, while the 1-4 interactions are scaled down by a factor of 0.5. Bond lengths were constrained by applying the LINCS algorithm⁷, a cutoff of 1.2 nm was applied to short-range dispersion interactions and the same distance for the particle-mesh Ewald method (PME)^{8,9} to take into account the long-range Coulomb electrostatics. Finally, a long-range dispersion correction term was added to both energy and pressure.

Table S2: Lennard-Jones parameters, point charges and atomic masses.

Site	Mass (a.u.)	q (a.u.)	σ (nm)	ε (kJ mol ⁻¹)
Ow	15.9994	-0.8476	0.31656	0.65019
Hw	1.0080	0.4238	0.0	0.0
N	14.0067	-0.900	0.330	0.711280
Nc	14.0067	-0.300	0.3250	0.711280
Nt	14.0067	0.000	0.3250	0.711280
Cn	12.0110	0.060	0.350	0.276144
Cnc	12.0110	0.190	0.350	0.276144
C	12.0110	-0.120	0.350	0.2761444
C3	12.0110	-0.180	0.350	0.2761444
Ct	12.0110	0.130	0.350	0.2761444
Hc	1.0080	0.060	0.250	0.125520
Hn	1.0080	0.360	0.0	0.0
Hnc	1.0080	0.330	0.0	0.0
Hcn	1.0080	0.060	0.250	0.06276
SiN	28.0855	1.3292	0.4435	0.39748
Cl	35.4530	-1.0	0.441724	0.492833
SiI	28.0855	1.0801	0.4435	0.39748
OhN	15.9994	-0.7641	0.34618	0.665674
OhI	15.9994	-0.7481	0.34618	0.665674
HoN	1.0080	0.4318	0.23541	0.413379
HoI	1.0080	0.3684	0.23541	0.413379
Oc	15.9994	-0.9410	0.34618	0.665674
ONN	15.9994	-0.6646	0.34506	0.67864
OII	15.9994	-0.7594	0.34506	0.67864
OIN	15.9994	-0.7120	0.34506	0.67864

Table S3: Bond lengths.

Bond	Lenght (nm)
Ow-Hw	0.100
N-Hn	0.101
N-Cn	0.1448
Nc-Hcn	0.101
Nc-Cnc	0.1471
Nt-Ct	0.1471
Cn-Hcn	0.109
Cn-C	0.1529
Cnc-Hc	0.109
Cnc-C	0.1529
C-Hc	0.109
C-C	0.1529
C3-C	0.1529
C3-Hc	0.1529
Ct-Hc	0.109
SiN-OhN	0.1652
SiI-OhI	0.1695
SiI-Oc	0.1581
SiN-ONN	0.1651
SiN-OIN	0.1651
SiI-OII	0.169
SiI-OIN	0.169
OhN-HoN	0.0968
OhI-HoI	0.0968

Table S4: Bond angles and harmonic force constants.

Angle	θ_0 (deg)	k_θ (kJ mol ⁻¹ rad ⁻²)
Hw-Ow-Hw	109.47	—
Hn-N-Hn	106.4	364.845
Hn-N-Cn	109.5	292.880
Hnc-Nc-Hnc	109.5	292.880
Hnc-Nc-Cnc	109.5	292.880
N-Cn-C	109.47	470.281
N-Cn-Hcn	109.5	292.880
Nc-Cnc-C	111.2	669.44
Nc-Cnc-Hcn	109.5	292.800
Nt-Ct-Hc	109.5	292.880
Hcn-Cn-Hcn	107.8	276.144
Hcn-Cn-C	110.7	313.800
Hcn-Cnc-Hcn	107.8	276.144
Hcn-Cnc-C	110.7	313.800
Cn-C-C	112.7	488.273
Cn-C-Hc	110.7	313.800
Cnc-C-C	112.7	488.273
Cnc-C-Hc	110.7	313.800
Ct-Nt-Ct	113.0	418.400
Hc-C-C	110.7	313.800
C3-C-Hc	110.7	313.800
C-C3-HC	110.7	313.800
Hc-C-Hc	107.8	276.144
Hc-C3-Hc	107.8	276.144
Hc-Ct-Hc	107.8	276.144
C-C-C	112.7	488.273
SiN-OhN-HoN	118.0442	109.29
SiI-OhI-HoI	118.0442	109.29
OhN-SiN-OhN	116.2621	255.64
OhI-SiI-OhI	116.2621	255.64
OhI-SiI-Oc	166.2621	255.64
SiN-ONN-SiN	174.2152	19.52
SiN-OIN-SiI	174.2152	19.52
SiI-OII-SiI	174.2152	19.52
OhN-SiN-ONN	111.0860	7343.28
OhN-SiN-OIN	111.0860	7343.28
OhI-SiI-OIN	111.0860	7343.28
OhI-SiI-OII	111.0860	7343.28
Oc-SiI-OIN	111.0860	7343.28
Oc-SiI-OII	111.0860	7343.28

Table S5: Dihedral torsion parameters.

Dihedral	C ₀ (kJ mol ⁻¹)	C ₁ (kJ mol ⁻¹)	C ₂ (kJ mol ⁻¹)	C ₃ (kJ mol ⁻¹)	C ₄ (kJ mol ⁻¹)	C ₅ (kJ mol ⁻¹)
Hn-N-Cn-Hcn	0.83680	2.51040	0.0	-3.34720	0.0	0.0
Hn-N-Cn-C	-1.26775	3.02085	1.74473	-3.49782	0.0	0.0
Hnc-Nc-Cnc-Hcn	0.54601	1.63803	0.0	-2.18405	0.0	0.0
Hnc-Nc-Cnc-C	-1.26775	3.02085	1.74473	-3.49782	0.0	0.0
N-Cn-C-Hc	-4.09614	5.08775	2.96645	-3.95806	0.0	0.0
N-Cn-C-C	3.33465	-1.5526	2.82001	-4.60240	0.0	0.0
Nc-Cnc-C-C	5.77183	-2.67148	0.95814	-4.05848	0.0	0.0
Nc-Cnc-C-Hc	0.8033	2.4099	0.0	-3.21331	0.0	0.0
Hcn-Cn-C-Hc	0.62760	1.88280	0.0	-2.51040	0.0	0.0
Hcn-Cn-C-C	0.62760	1.88280	0.0	-2.51040	0.0	0.0
Hcn-Cnc-C-Hc	0.62760	1.88280	0.0	-2.51040	0.0	0.0
Hc-C-C-Hc	0.62760	1.88280	0.0	-2.51040	0.0	0.0
Hc-C-C3-Hc	0.62760	1.88280	0.0	-2.51040	0.0	0.0
Hcn-Cnc-C-C	0.62760	1.88280	0.0	-2.51040	0.0	0.0
Hc-Ct-Nt-Ct	0.63179	1.89535	0.0	-2.52714	0.0	0.0
Cn-C-C-C	2.92880	-1.46440	0.20920	-1.67360	0.0	0.0
Cnc-C-C-C	2.92880	-1.46440	0.20920	-1.67360	0.0	0.0
C-C-C-C	2.92880	-1.46440	0.20920	-1.67360	0.0	0.0
OhN-SiN-OhN-HoN	14.8473	9.1554	-3.6233	2.0686	0.0	0.0
OhI-SiI-OhI-HoI	14.8473	9.1554	-3.6233	2.0686	0.0	0.0
Oc-SiI-OhI-HoI	14.8473	9.1554	-3.6233	2.0686	0.0	0.0
ONN-SiN-OhN-HoN	15.2038	23.8622	-2.5673	-9.8910	0.0	0.0
OIN-SiN-OhN-HoN	15.2038	23.8622	-2.5673	-9.8910	0.0	0.0
OII-SiI-OhI-HoI	15.2038	23.8622	-2.5673	-9.8910	0.0	0.0
OIN-SiI-OhI-HoI	15.2038	23.8622	-2.5673	-9.8910	0.0	0.0
OhN-SiN-ONN-SiN	-3.3698	-4.0041	-0.6343	0.0	0.0	0.0
OhN-SiN-OIN-SiI	-3.3698	-4.0041	-0.6343	0.0	0.0	0.0
OhI-SiI-OII-SiI	-3.3698	-4.0041	-0.6343	0.0	0.0	0.0
OhI-SiI-OIN-SiN	-3.3698	-4.0041	-0.6343	0.0	0.0	0.0
Oc-SiI-OII-SiI	-3.3698	-4.0041	-0.6343	0.0	0.0	0.0
Oc-SiI-OIN-SiN	-3.3698	-4.0041	-0.6343	0.0	0.0	0.0

Initial configurations for all-atom (AA) simulations were created by placing in the center of the simulation box a preformed micelle consisting of 70 surfactants (charged or neutral). The preformed micelle was made using the software Packmol¹⁰ and its size chosen to match, approximately, the experimentally measured aggregation number for the system, in the absence of silica, at 50 °C¹¹. In the next step, counter-ions, i.e. chloride (Cl⁻) and tetramethylammonium (TMA⁺), as well as silica monomers and dimers were randomly added to

the box and the system solvated with a fixed number of water molecules. The original reacting mixture for HMS materials contains also ethanol, however, to reduce the complexity of the simulations this was neglected and replaced by water, as done previously in modelling the synthesis of MCM-41^{6,12,13}. All atomistic simulations performed are listed in Table S6, however it should be noted that only the systems marked with an asterisk have been presented and discussed explicitly in the main body of this work. The remainder have also been included since they were used to develop the CG model, as will be later discussed in Section 3 of this document.

Table S6: Number of molecules in each atomistic MD simulation of preformed aggregates used to develop parameters of the coarse-grained model. Only simulations marked with (*) are discussed in the main body of this work. DDA⁺, charged surfactant; DDA, neutral surfactant; Cl⁻, chloride ion; TMA⁺, tetramethylammonium ion; SI, anionic silica monomer; SN, neutral silica monomer; SISI, silica dimer with two charges; SISN, silica dimer with one charge; SNSN, neutral silica dimer, and water. The final box size is approximately 8.1 nm in all directions.

System	DDA ⁺	DDA	Cl ⁻	TMA ⁺	SI	SN	SISI	SISN	SNSN	water
(*) AA-DDA ⁺	70		70							16420
AA-DDA ⁺ /SI	70				70					16420
AA-DDA ⁺ /SN	70		70			70				16420
(*) AA-DDA ⁺ /SI/SN	70				70	70				16420
AA-DDA ⁺ /SISI	70						35			16420
AA-DDA ⁺ /SISN	70		35					35		16420
AA-DDA ⁺ /SNSN	70		70						35	16420
AA-DDA		70								16420
(*) AA-DDA/SN		70				70				16420
AA-DDA/SI		70		70	70					16420
AA-DDA/SN/SI		70		70	70	70				16420

For each AA system studied, an energy minimisation step followed by two short equilibration steps (first *NVT* and then *NPT*) were performed. Then, the system was run for production at 323 K in the *NPT* ensemble for at least 10 ns. The temperature was kept constant using the Nosé-Hoover thermostat¹⁴ and the pressure fixed at 1 bar employing the Parrinello-Rahman barostat¹⁵. The equations of motion were integrated using the leap-frog algorithm¹⁶ with a time step of 2 fs. The simulation boxes were always cubic with periodic

boundary conditions applied in x, y and z directions.

3 Coarse-grained simulations

Two types of coarse-grained (CG) simulations were considered: i) simulations of small systems consisting of preformed micelles in solution with counter-ions and/or silicates, used to develop and validate the CG interaction parameters and ii) simulations of large systems starting from random distributions of all species in solution, used to investigate the mechanism of formation of HMS materials.

CG model development The small systems, used to develop our CG model, were created similarly to the atomistic ones by placing a preformed micelle of CG surfactants in the center of a simulation box of approximately 8 nm (see Table S7). In the next step, all other species were added and the system solvated with a pre-equilibrated box of CG water. The number of CG water beads used in each system was adjusted to match the concentration of the corresponding AA simulation, taking into account that in the MARTINI force field¹⁷ a CG chloride ion includes its solvation shell (made of 6 atomistic water molecules), and that a single water bead corresponds to 4 atomistic water molecules. Another feature of the MARTINI model for water is that it tends to undergo freezing at ambient temperature, so it is normally recommended to replace 10 % of the water with so-called antifreeze (AF) particles (BP₄ type beads) to avoid this issue. With regard to this work, no antifreeze particles were included since the temperature used in our simulations (50 °C) is considerably above the freezing temperature of the MARTINI model for water.

The approach used to develop our CG parameters is based on the methodology employed by Pérez-Sánchez et al. to obtain their CG model of MCM-41 formation¹⁸. This involved comparing density profiles of preformed aggregates of the same size obtained from AA and CG simulations, and subsequently tuning such interactions at the CG level until the best set of parameters reproducing the AA results was found¹⁸. Specifically, the final set of

Table S7: Number of molecules in each coarse-grained MD simulation of preformed aggregates used to develop parameters of the coarse-grained model. DDA⁺, charged surfactant; DDA, neutral surfactant; Cl⁻, chloride ion; TMA⁺, tetramethylammonium ion; SI, anionic silica monomer; SN, neutral silica monomer; SISI, silica dimer with two charges; SISN, silica dimer with one charge; SNSN, neutral silica dimer, and water. The final box size is approximately 8.1 nm in all directions.

System	DDA ⁺	DDA	Cl ⁻	TMA ⁺	SI	SN	SISI	SISN	SNSN	water
AA-DDA ⁺	70		70							4000
AA-DDA ⁺ /SI	70				70					4105
AA-DDA ⁺ /SN	70		70			70				4000
AA-DDA ⁺ /SI/SN	70				70	70				4105
AA-DDA ⁺ /SISI	70						35			4105
AA-DDA ⁺ /SISN	70		35					35		4053
AA-DDA ⁺ /SNSN	70		70						35	4000
AA-DDA		70								4105
AA-DDA/SN		70				70				4105
AA-DDA/SI		70		70	70					4105
AA-DDA/SN/SI		70		70	70	70				4105

parameters was obtained in a progressive manner by gradually including more species into our simulations, hence allowing, at each step, to validate the previously obtained parameters.

Prior to the production runs, the CG systems were energy minimised, followed by a short relaxation step. Production simulations were then performed in the *NPT* ensemble for up to 40 ns by keeping the temperature constant at 323 K using the velocity-rescaling thermostat¹⁹ and the pressure fixed at 1 bar using the Parrinello-Rahman barostat¹⁵. The equations of motion were integrated using the the leap-frog algorithm¹⁶ with a time step of 40 fs, and cubic periodic boundary conditions were applied in all directions.

Trajectories were then analysed using an adaptation of the Hoshen-Kopelman cluster-counting algorithm²⁰. For this purpose, two surfactant molecules were considered part of the same cluster if, at the atomistic level, the distance between the last four atoms (one carbon and three hydrogens), or, at coarse-grained level, the distance between the last tail beads, was less than 0.75 nm. This value was chosen since it is close to the position of the first minimum in the respective radial distribution functions. The equation used to compute

the number-average cluster size for clusters larger than 4 molecules is:

$$\langle CN_N \rangle_4 = \frac{\sum_{n=4}^{\infty} n[M_n]}{\sum_{n=4}^{\infty} [M_n]} \quad (1)$$

where n indicates the size of the clusters and M_n the concentration of clusters with n molecules. The cluster-counting algorithm allowed us to calculate AA and CG average density profiles, measured from the micelle centre of mass (COM). It should be noted that the standard mass of a MARTINI bead is 72 a.u.; however, for the purpose of the density profile calculation, real masses were attributed to each bead to match the corresponding atomistic group (i.e. head, tail, monomer, dimers, etc.). For example the mass of the bead representing the charged head is approximately 17 a.u. (i.e. the mass of one nitrogen and three hydrogens), while the mass of the SN bead is approximately 96 a.u. (i.e. the mass of one silicon atom, four oxygens and four hydrogens), etc.. Figure S5 displays a schematic representation of the mapping scheme adopted for each species considered.

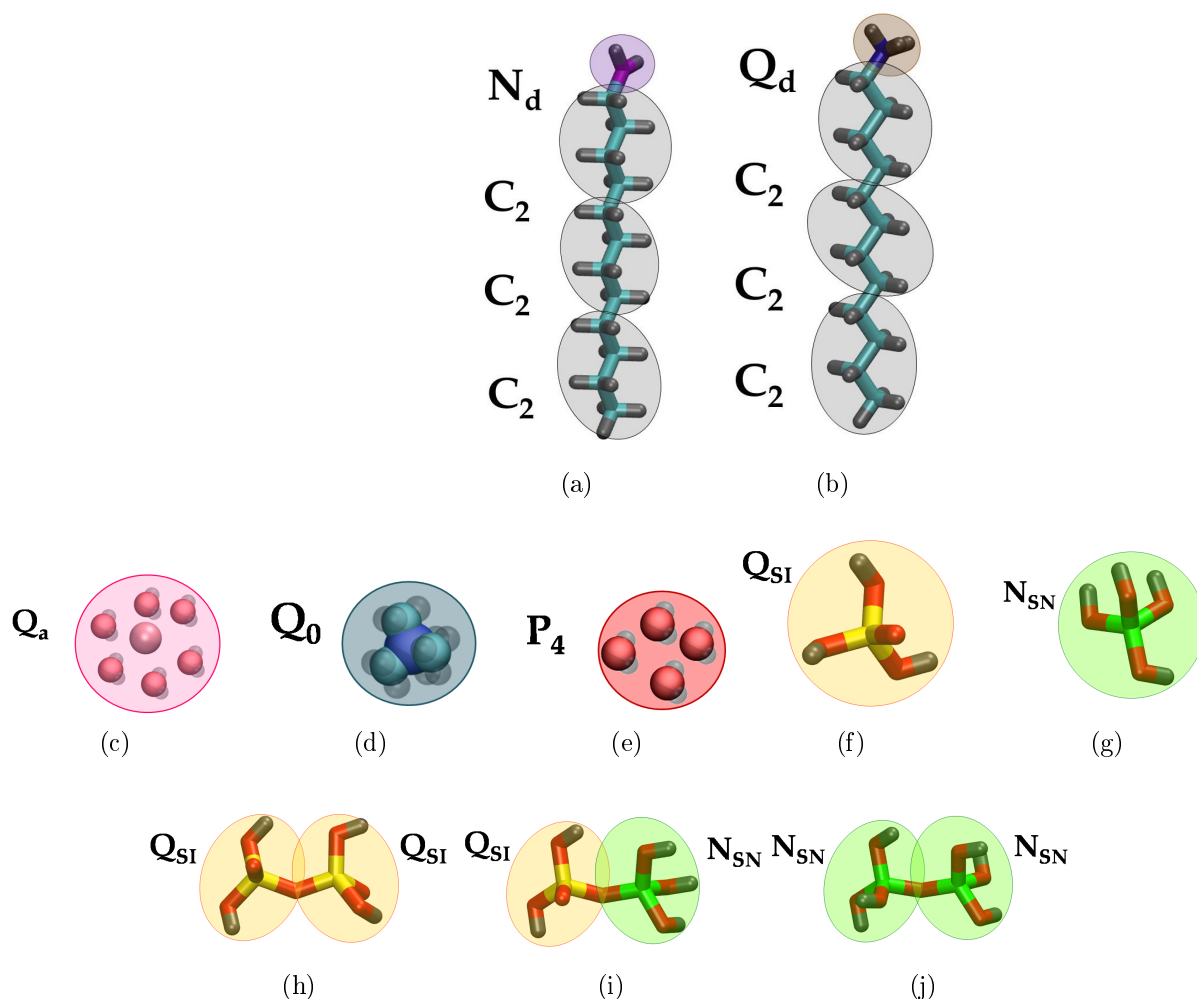


Figure S5: Schematic representation of the CG mapping schemes adopted in this work. DDA surfactant, (a); DDA^+ , (b); solvated chloride counter-ions, (c); TMA^+ counter-ions, (d); water, (e); anionic silica monomer, (f); neutral silica monomer, (g); doubly deprotonated dimer, (h); singly deprotonated dimer, (i) and neutral dimer, (j).

In the following, CG density profiles and representative snapshots obtained by employing this methodology are presented in comparison to the corresponding AA systems (see Figures S6-S14).

In order to improve structural agreement between AA and CG micelle density profiles, a higher angle force constant than the standard MARTINI value (50 kJ mol^{-1} instead of 25 kJ mol^{-1}) was used to model surfactant beads, charged or neutral. This was shown to produce narrower surfactant head profiles as well as steeper tail and water distributions. It

should be noted that higher values of the angle force constant (up to $f = 500 \text{ kJ mol}^{-1}$) were also tested producing even better agreement with AA results. However, when these very high angle force constant values were employed to model large systems at high surfactant concentration, freezing was observed to take place due to the extreme rigidity of the model. We attribute the discrepancies between AA and CG profiles for chloride counter-ions (pink curves in Figure S6, Figure S13 and Figure S14) to the larger size of the ion at CG level. In fact, by including also a solvation shell, in the CG bead, chloride ions are not allowed to adsorb as close to the surfactant heads as they do at atomistic level. Furthermore, neutral micelles appear to be more disordered than charged ones: some of the head groups are located inside the micelle core and some water molecules can penetrate inside it (see Figure S7). Since neutral DDA surfactants cannot dissolve in pure water²¹, the presence of head groups in the core of the neutral micelles is an indication that, at these conditions, micelles are not the thermodynamically stable aggregation state (see Figure 2-b of the main paper). Nevertheless, also in this regard, AA and CG models show the same qualitative behaviour.

For the system containing silica monomers and dimers, we notice that although the height of the density peaks is not exactly captured by the CG model, the position and width of both silica and head group peaks is in general matched quite well with the AA profiles. We attribute the small discrepancies between CG and AA profiles to the more disordered nature of CG surfactant micelles, brought about by the lower resolution of the model.

The final set of CG parameters is summarised in Table S8.

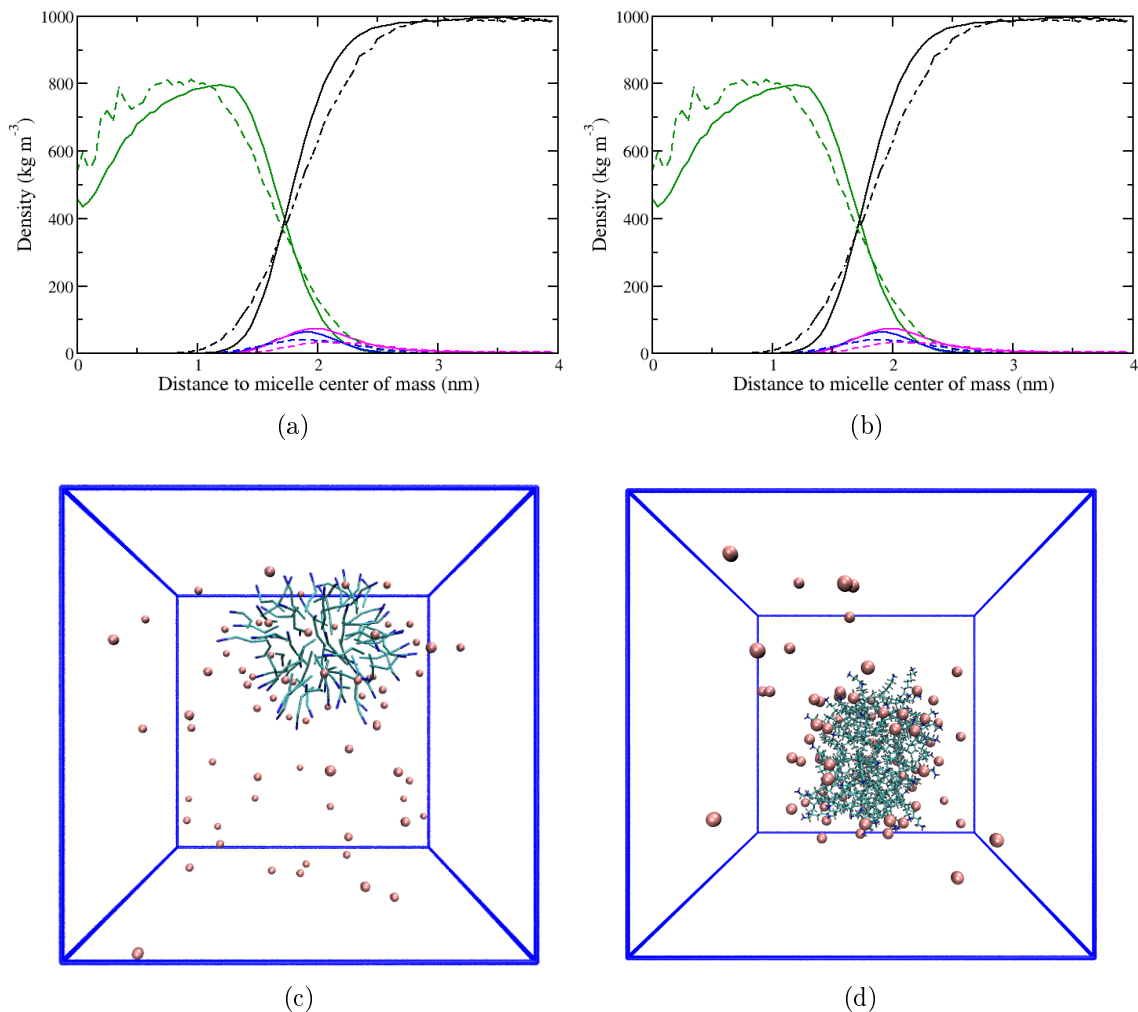


Figure S6: Top: (a)-(b), Comparison between atomistic (solid lines) and coarse-grained (dashed lines) average micelle density profiles obtained for the reference system with DDA⁺ surfactants and Cl⁻ ions. The angle force constant is set to $f = 50 \text{ kJ mol}^{-1}$ the CG surfactant. Tails, dark green; charged heads, blue; chloride ions, pink and water, black. Bottom: (c)-(d), Snapshots comparing the final configurations obtained with coarse-grained (c) and atomistic (d) simulations for the same system. Colour code for the CG snapshot is: charged heads, blue and tails, teal. Colour code for the AA snapshot is: charged nitrogens, blue; carbons, teal; hydrogens, grey and chloride ions, pink. Water has been removed for clarity.

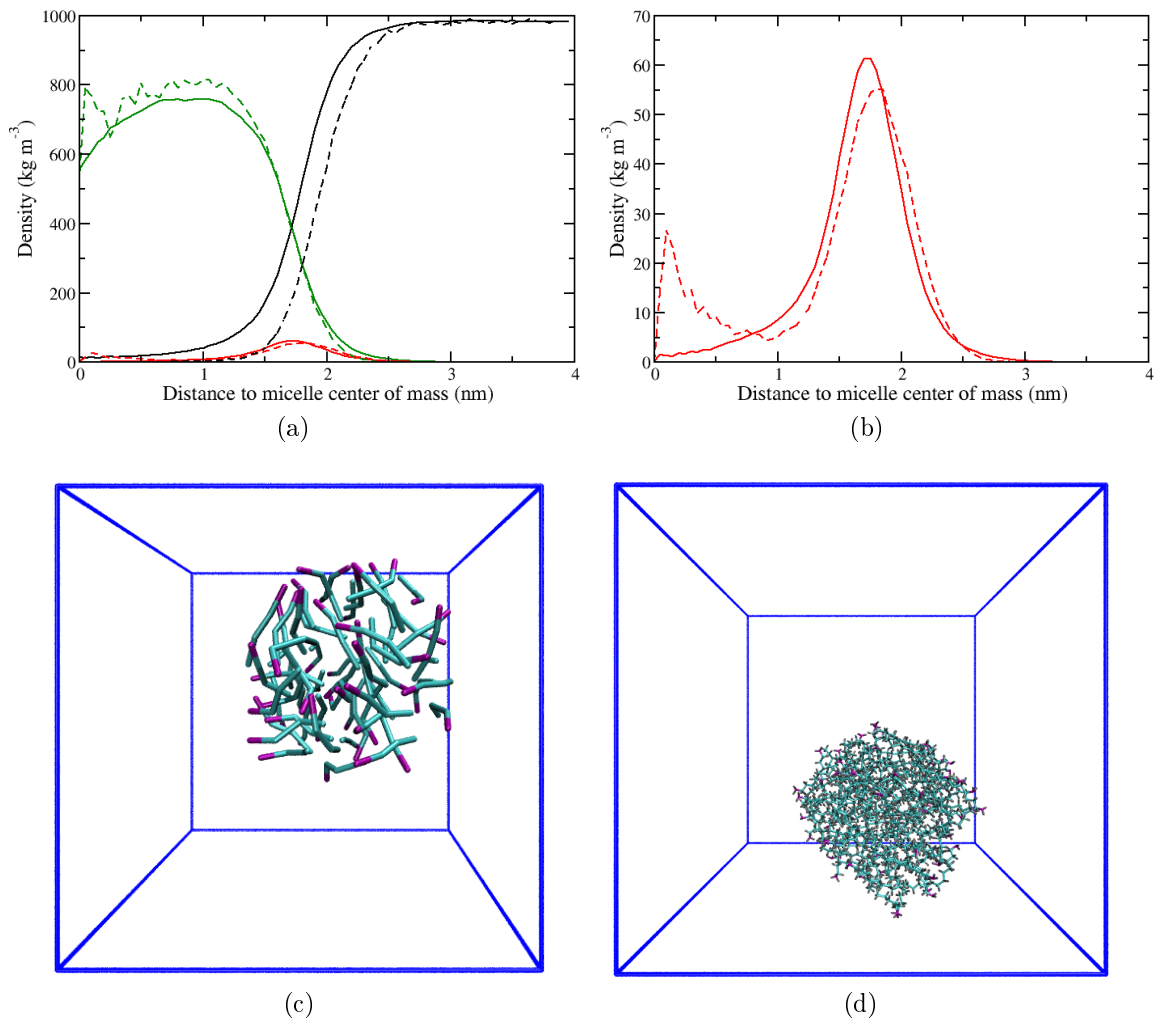


Figure S7: Top: (a)-(b), Comparison between atomistic (solid lines) and coarse-grained (dashed lines) average micelle density profiles obtained for the reference system with DDA surfactants. The angle force constant is set to $f = 50 \text{ kJ mol}^{-1}$ the CG surfactant. Tails, dark green; neutral heads, red and water, black. Bottom: (c)-(d), Snapshots comparing the final configurations obtained with coarse-grained (c) and atomistic (d) simulations for the same system. Colour code for the CG snapshot is: neutral heads, purple and tails, teal. Colour code for the AA snapshot is: neutral nitrogens, purple; carbons, teal and hydrogens, grey. Water has been removed for clarity.

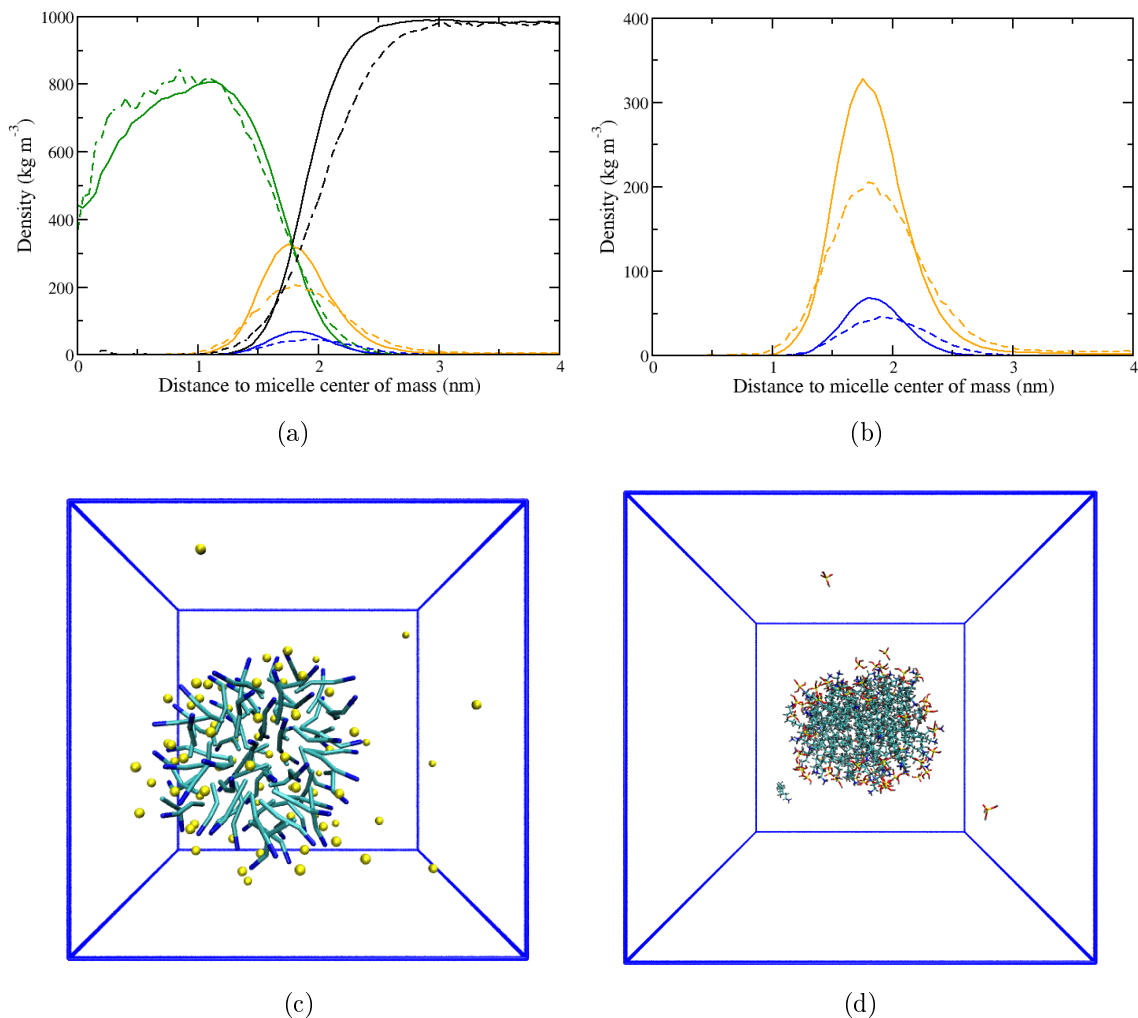


Figure S8: Top: (a)-(b), Comparison between atomistic (solid lines) and coarse-grained (dashed lines) average micelle density profiles obtained for the system containing DDA⁺ surfactants and SI monomers ($Q_{SI}-Q_d = II$). Tails, dark green; charged heads, blue; anionic silica monomers, yellow and water, black. Bottom: (c)-(d), Snapshots comparing the final configurations obtained with coarse-grained (c) and atomistic (d) simulations for the same system. Colour code for the CG snapshot is: charged heads, blue; tails, teal and SI monomers, yellow. Colour code for the AA snapshot is: charged nitrogens, blue, carbons, teal, hydrogens, grey; oxygens, red and charged silicons, yellow. Water has been removed for clarity.

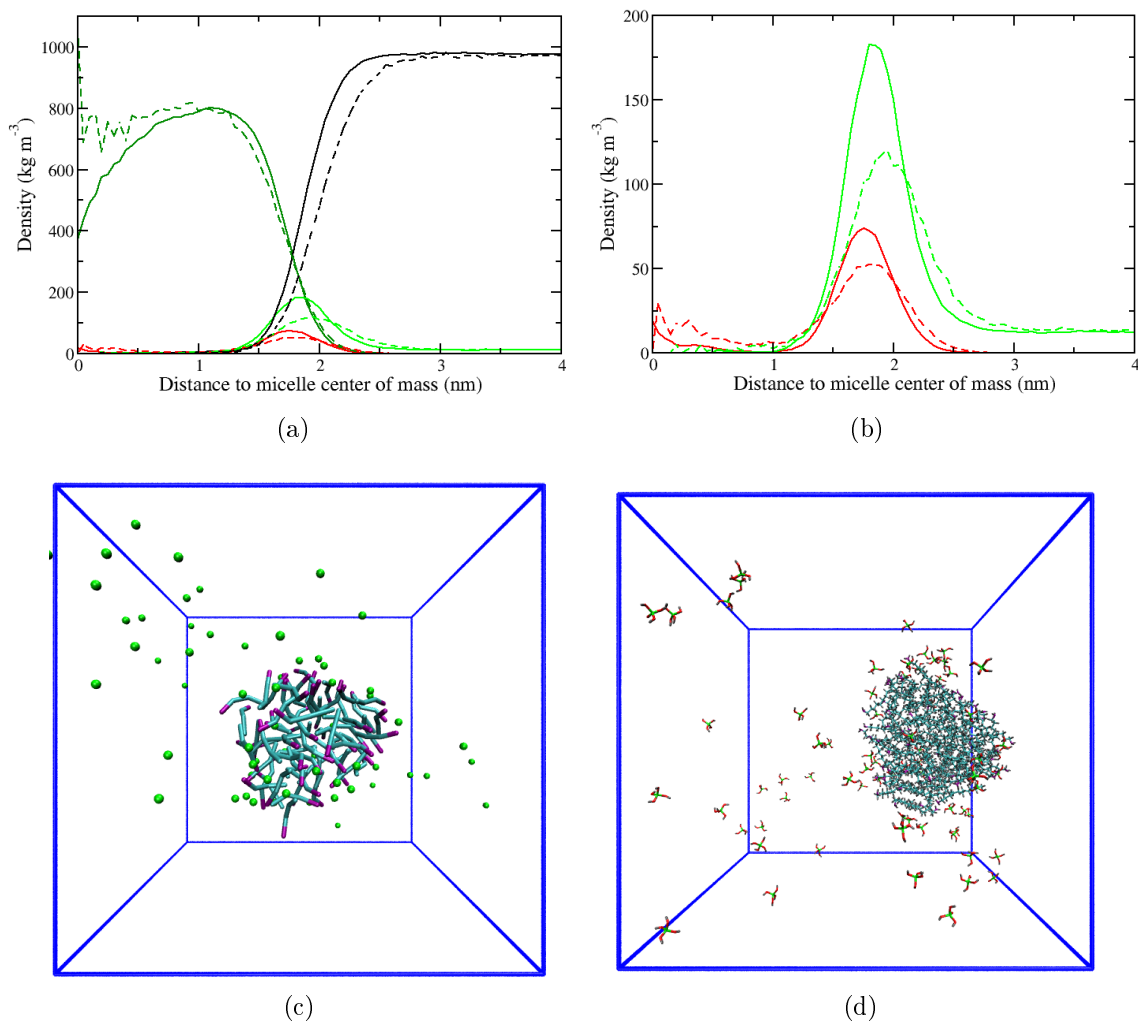


Figure S9: Top: (a)-(b), Comparison between atomistic (solid lines) and coarse-grained (dashed lines) average micelle density profiles obtained for the system containing DDA surfactants and SN monomers ($N_{SN}-N_d=0$). Tails, dark green; neutral heads, red; neutral silica monomers, green and water, black. Bottom: (c)-(d), Snapshots comparing the final configurations obtained with coarse-grained (c) and atomistic (d) simulations for the same system. Colour code for the CG snapshot is: neutral heads, purple; tails, teal and SN monomers is green. Colour code for the AA snapshot is: neutral nitrogens, purple; carbons, teal; hydrogens, grey; oxygens, red and neutral silicons, green. Water has been removed for clarity.

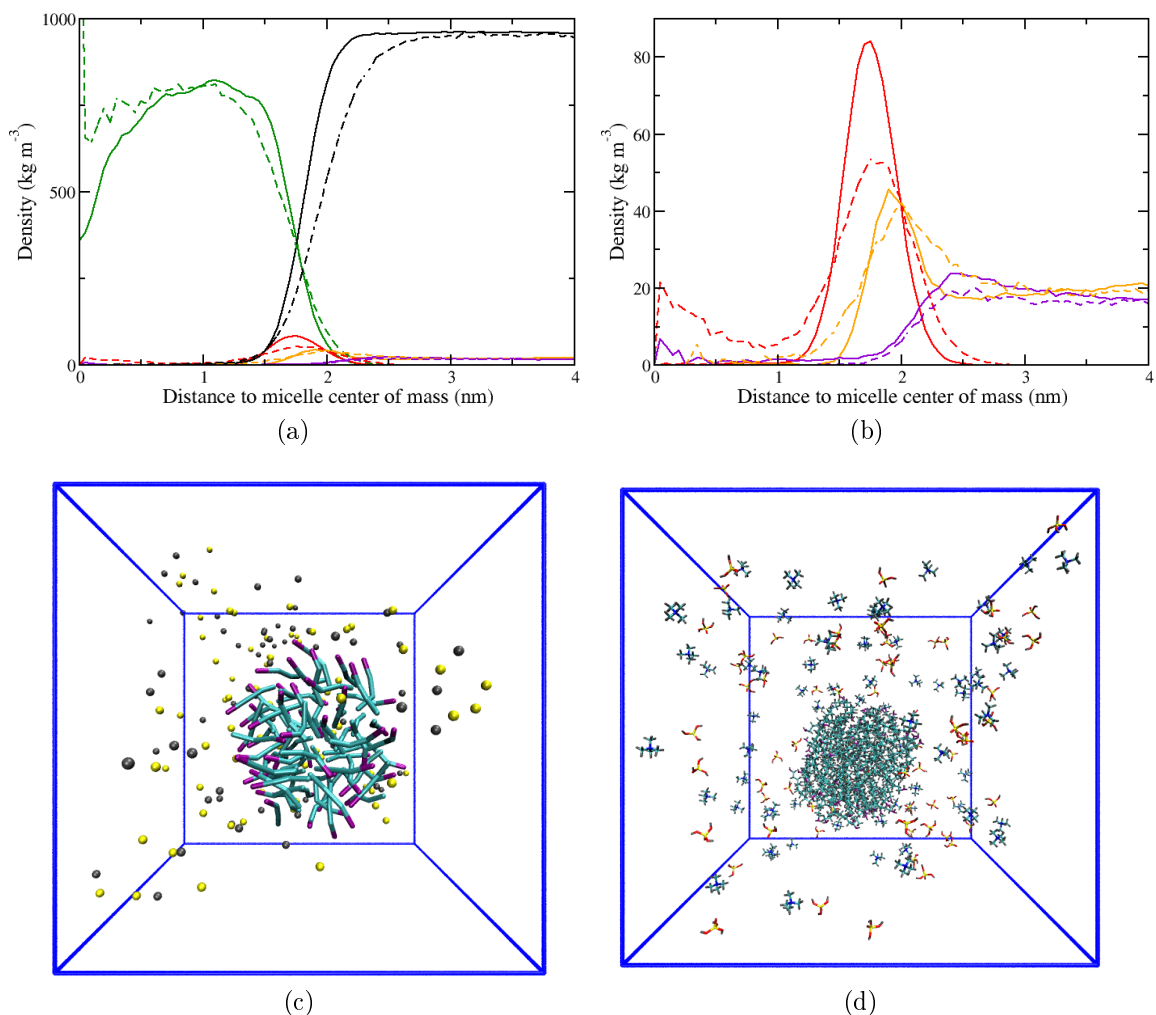


Figure S10: Top: (a)-(b), Comparison between atomistic (solid lines) and coarse-grained (dashed lines) average micelle density profiles obtained for the system containing DDA surfactants, SI monomers and TMA counter-ions ($Q_{SI}-N_d = III$). Tails, dark green; neutral heads, red; anionic silica monomers, yellow; TMA counter-ions, purple and water, black. Bottom: (c)-(d), Snapshots comparing the final configurations obtained with coarse-grained (c) and atomistic (d) simulations for the same system. Colour code for the CG snapshot is: neutral heads, purple; tails, teal; SI monomers, yellow and TMA counter-ions grey. Colour code for the AA snapshot is: neutral nitrogens, purple, carbons, teal, hydrogens, grey; oxygens, red and charged silicons, yellow. Water has been removed for clarity. Water has been removed for clarity.

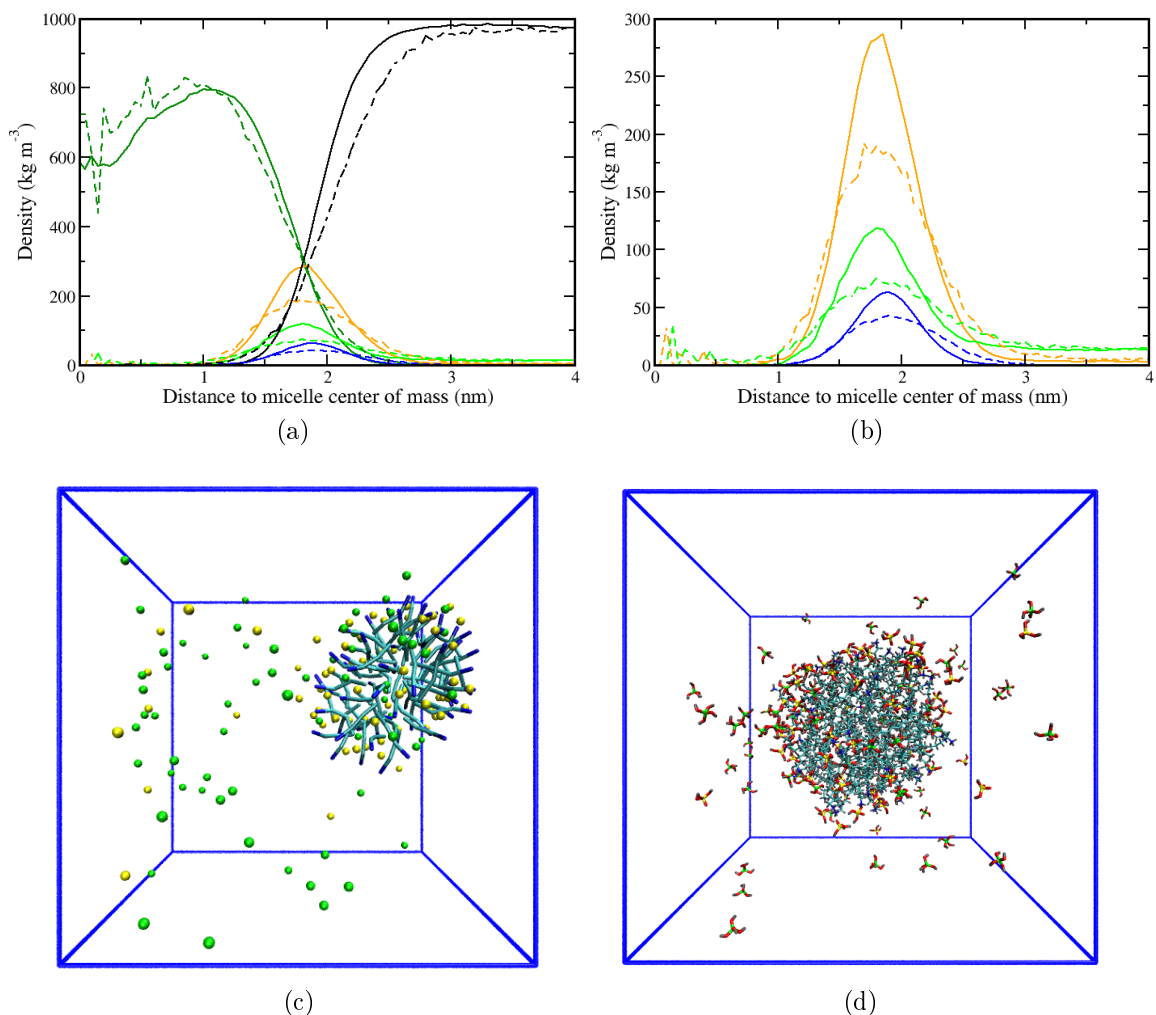


Figure S11: Top: (a)-(b), Comparison between atomistic (solid lines) and coarse-grained (dashed lines) average micelle density profiles obtained for the system containing DDA^+ surfactants and both SI and SN monomers ($Q_{SI}-N_{SN} = 0$ and $N_{SN}-Q_d = 0$). Tails, dark green; charged heads, blue; anionic silica monomers, yellow; neutral silica monomers, green and water, black. Bottom: (c)-(d), Snapshots comparing the final configurations obtained with coarse-grained (c) and atomistic (d) simulations for the same system. Colour code for the CG snapshot is: charged heads, blue; tails, teal; SI monomers, yellow and SN monomers is green. Colour code for the AA snapshot is: charged nitrogens, blue, carbons, teal, hydrogens, grey; oxygens, red; charged silicons, yellow and neutral silicons, green. Water has been removed for clarity.

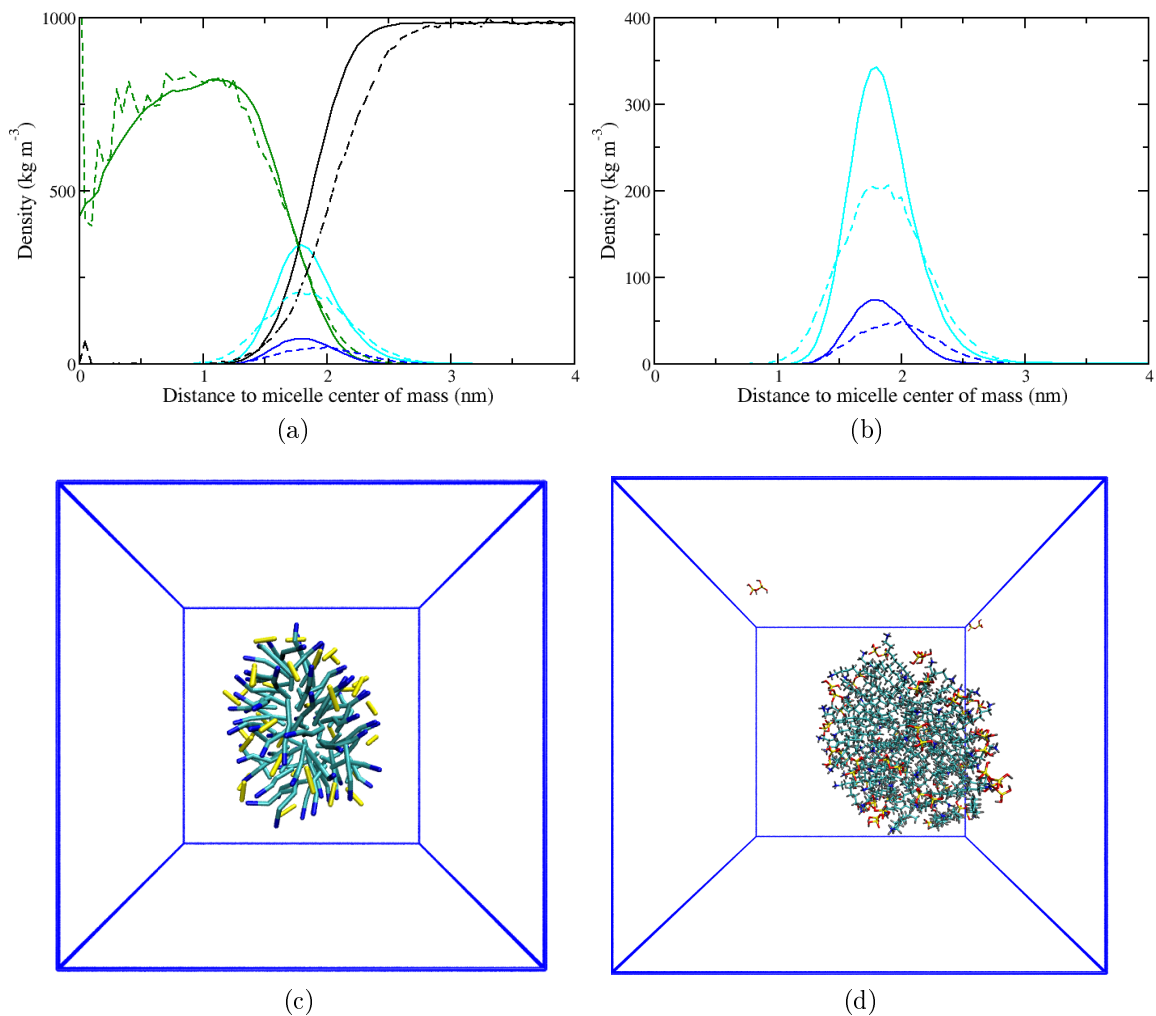


Figure S12: Top: (a)-(b), Comparison between atomistic (solid lines) and coarse-grained (dashed lines) average micelle density profiles obtained for the system containing DDA^+ surfactants and SISI dimers. The SISI dimer is represented by two Q_{SI} beads. Tails, dark green; charged heads, blue; SISI dimers, cyan and water, black. Bottom: (c)-(d), Snapshots comparing the final configurations obtained with coarse-grained (c) and atomistic (d) simulations for the same system. Colour code for the CG snapshot is: charged heads, blue; tails, teal and SISI dimers, yellow. Colour code for the AA snapshot is: charged nitrogens, blue; carbons, teal; hydrogens, grey; oxygens, red and charged silicons, yellow. Water has been removed for clarity.

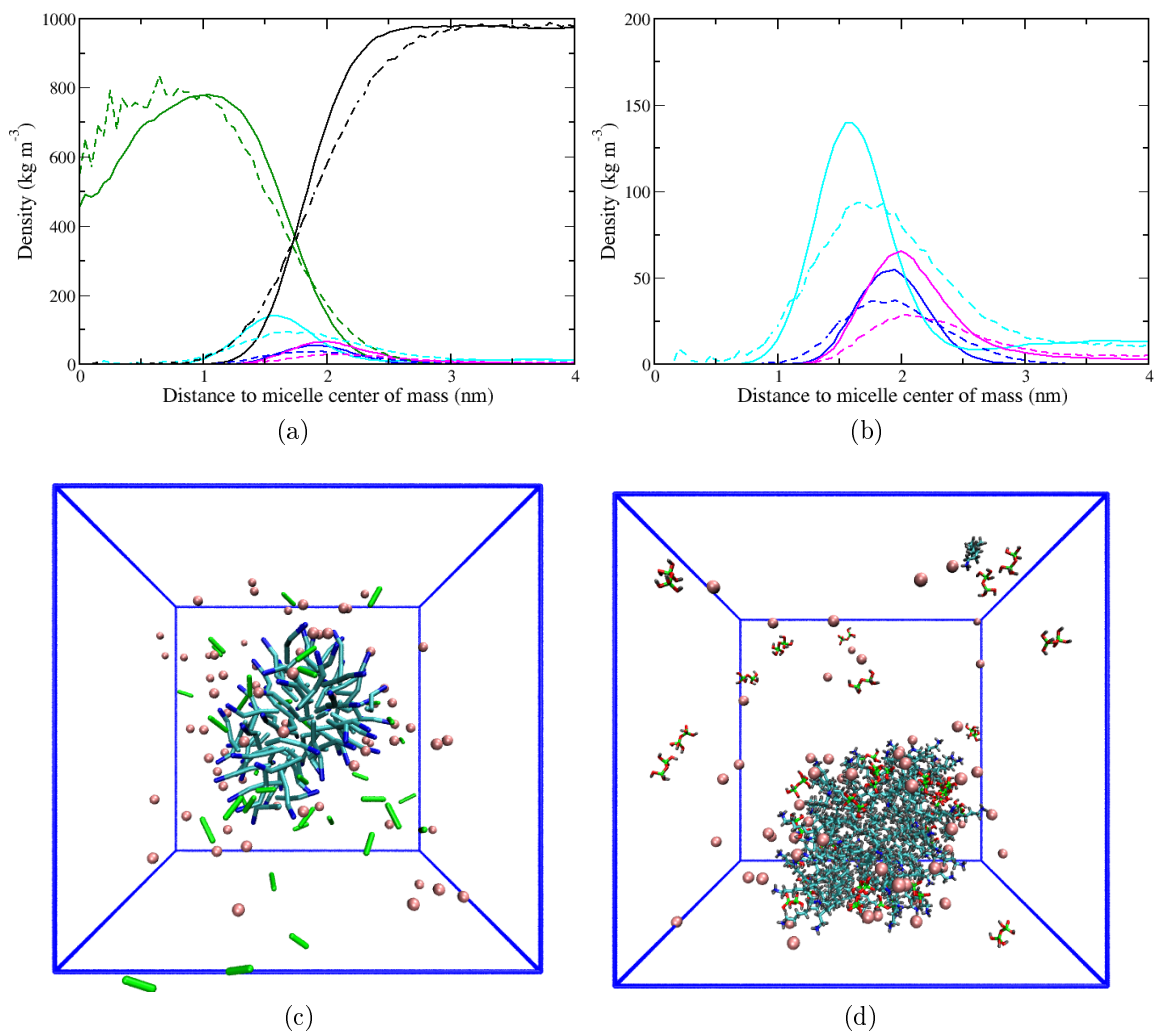


Figure S13: Top: (a)-(b), Comparison between atomistic (solid lines) and coarse-grained (dashed lines) average micelle density profiles obtained for the system containing DDA⁺ surfactants, SNSN dimers and Cl ions. The SNSN dimer is represented by two N_{SN} beads. Tails, dark green; charged heads, blue; SNSN dimers, cyan; chloride ion, purple and water, black. Bottom: (c)-(d), Snapshots comparing the final configurations obtained with coarse-grained (c) and atomistic (d) simulations for the same system. Colour code for the CG snapshot is: charged heads, blue; tails, teal, SNSN dimers, green and Cl ions, pink. Colour code for the AA snapshot is: charged nitrogens, blue, carbons, teal, hydrogens, grey; oxygens, red and neutral silicons, green. Water has been removed for clarity.

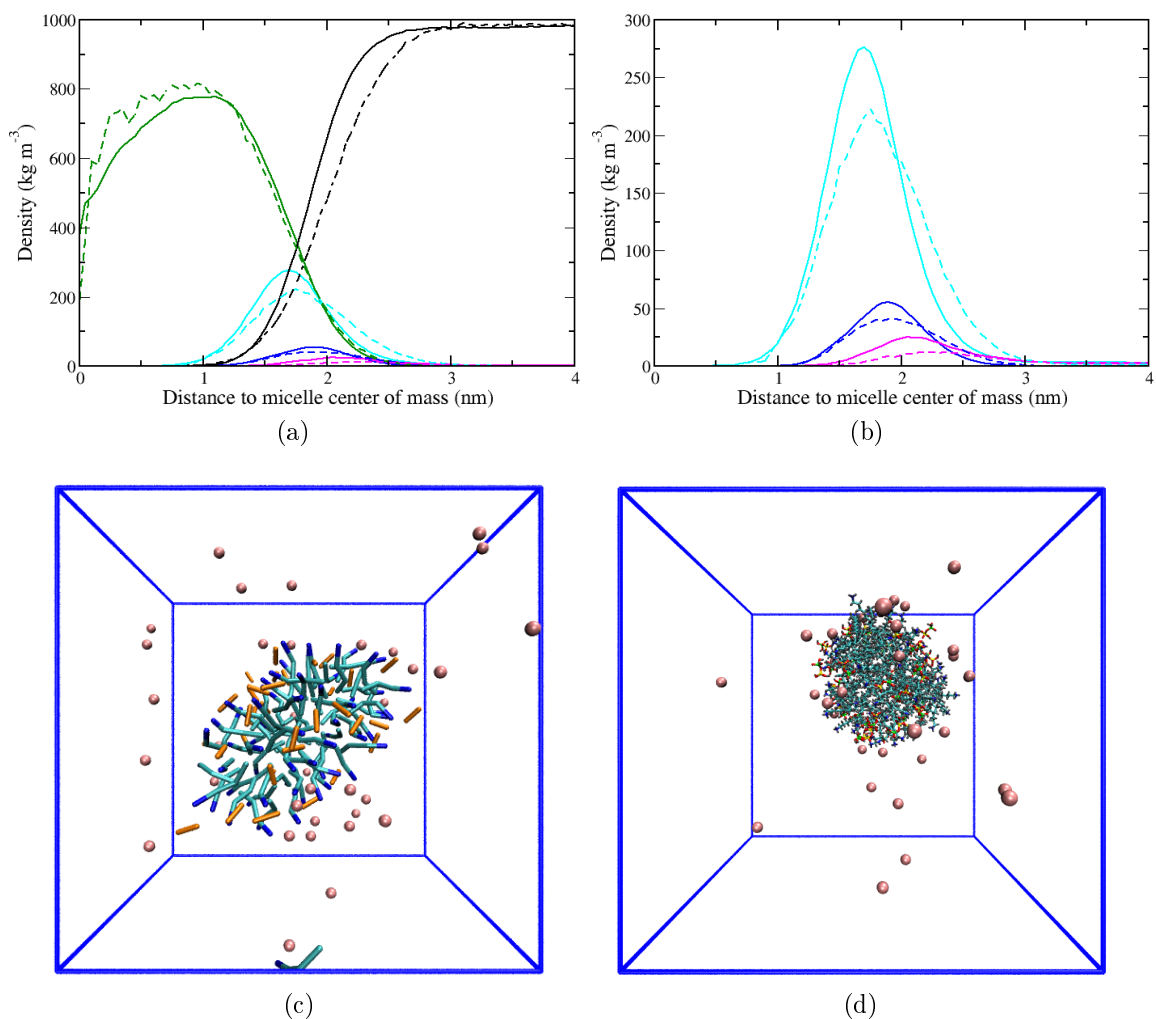


Figure S14: Top: (a)-(b), Comparison between atomistic (solid lines) and coarse-grained (dashed lines) average micelle density profiles obtained for the system containing DDA⁺ surfactants, SISN dimers and Cl ions. The SISN dimer is represented by one Q_{SI} and one N_{SN} beads. Tails, dark green; charged heads, blue; SISN dimers, cyan; chloride ion, purple and water, black. Bottom: (c)-(d), Snapshots comparing the final configurations obtained with coarse-grained (c) and atomistic (d) simulations for the same system. Colour code for the CG snapshot is: charged heads, blue; tails, teal, SISN dimers, orange and Cl ions, pink. Colour code for the AA snapshot is: charged nitrogens, blue; carbons, teal; hydrogens, grey; oxygens, red; charged silicons, yellow and neutral silicons, green. Water has been removed for clarity.

Table S8: Interaction matrix for CG beads used in this work. The notation follows the original MARTINI paper¹⁷: 0 - *supra attractive* ($\epsilon = 5.6$ kJ mol⁻¹), I - *attractive* ($\epsilon = 5.0$ kJ mol⁻¹), II - *almost attractive* ($\epsilon = 4.5$ kJ mol⁻¹), III - *semi attractive* ($\epsilon = 4.0$ kJ mol⁻¹), IV - *intermediate* ($\epsilon = 3.5$ kJ mol⁻¹), V - *almost intermediate* ($\epsilon = 3.1$ kJ mol⁻¹), VI - *semi repulsive* ($\epsilon = 2.7$ kJ mol⁻¹), VII - *almost repulsive* ($\epsilon = 2.3$ kJ mol⁻¹), VIII - *repulsive* ($\epsilon = 2.0$ kJ mol⁻¹), IX - *supra repulsive* ($\epsilon = 2.0$ kJ mol⁻¹). The value of σ is set to 0.47 nm for all levels of interactions except for level IX for which it is set to 0.62 nm.

Type	Q _d	Q _a	Q _o	Q _{SI}	P ₄	N _d	N _{SN}	C ₂
Q _d	I	0	II	II	0	III	0	IX
Q _a	0	I	II	II	0	I	II	IX
Q _o	II	II	IV	II	0	III	II	IX
Q _{SI}	II	II	II	0	II	III	0	IV
P ₄	0	0	0	II	I	III	II	VII
N _d	III	I	III	III	III	III	0	VI
N _{SN}	0	II	II	0	II	0	0	IV
C ₂	IX	IX	IX	IV	VII	VI	IV	IV

Simulations of HMS materials synthesis Large CG simulations used to investigate the synthesis of HMS materials at different pH conditions were performed in the *NPT* ensemble fixing temperature at 50 °C, pressure at 1 bar and following exactly the same simulation protocol used for the small CG systems used in the model development. Table S9 provides a list of all the simulations performed.

Table S9: Number of beads, simulation length and final box size for each coarse-grained MD simulation of HMS materials.

System	DDA ⁺	DDA	Cl ⁻	SI	SN	TMA ⁺	SISI	SISN	SNSN	water	time (ns)	box (nm)
DDA ⁺	1000		1000							61636	1200	20.1
DDA		1000								63136	600	20.1
DDA ⁺ + SI	1000			1000						63136	1200	20.2
DDA + SI		1000		1000		1000				63136	600	20.3
DDA + SN		1000			1000					63136	600	20.2
DDA ⁺ + SI + SN	1000		770	230	770					63136	2400	20.3
DDA ⁺ + DDA + SI + SN	890	110	660	230	770					63136	2400	20.3
DDA ⁺ + 1t01 SISN + SNSN	1000		880					120	380	61816	3000	20.2
DDA ⁺ + 2t01 SISN + SNSN	1000		760					240	760	61996	1800	20.3
DDA ⁺ + 3t01 SISN + SNSN	1000		640					360	1400	62176	600	20.4
DDA ⁺ + 4t01 SISN + SNSN	1000		520					480	1520	62356	1200	20.4

4 Additional results

The monomeric solution at pH ~ 9.2 Figure S15 shows a comparison of the final snapshots obtained when simulating the monomeric solution at the measured pH of 9.2 (approximately corresponding to 23 % anionic silica monomers and 77 % neutral silica monomers) with 100 % charged DDA surfactants (Figure S15-a) and with respectively 89 % charged and 11 % neutral DDA surfactants (Figure S15-b).

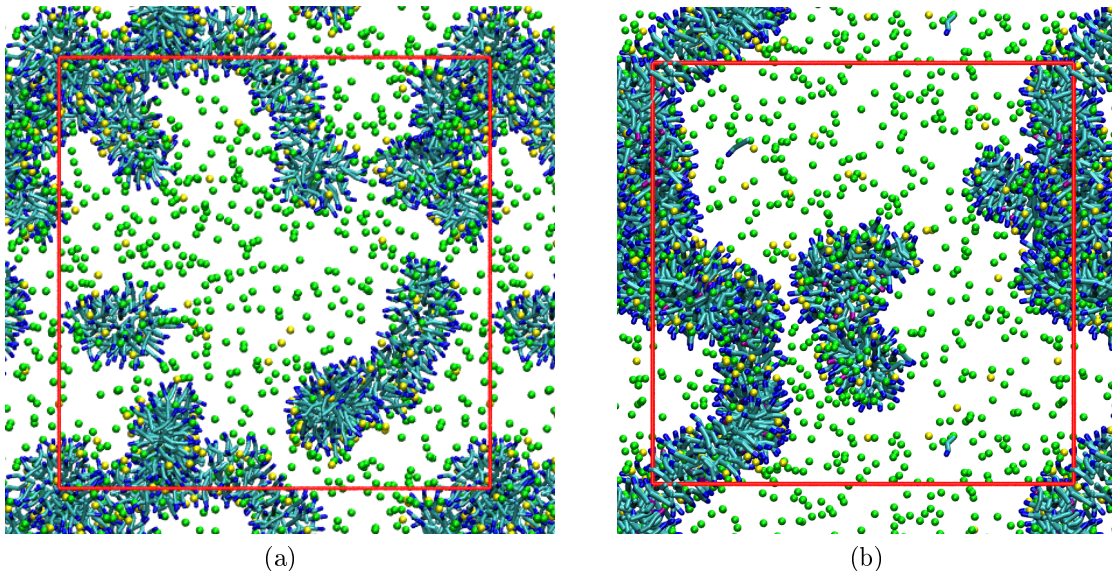


Figure S15: Simulation snapshots obtained for aqueous DDA solutions at 0.22 M with 23 % anionic silica monomers and 77 % neutral silica monomers (pH ~ 9.2): (a) with 100 % charged surfactants and (b) with 89 % charged and 11 % neutral surfactants. Water has been removed for clarity. Parts of the periodic images have been included to aid visualisation. Colour code is: charged heads, blue; neutral heads, purple; tails, teal; SI monomers, yellow; SN monomers, green.

Number of contacts To show that anionic silicates preferentially interact with surfactant head groups, we have calculated the number of contacts between surfactants and silicate species for the system containing charged surfactants and both charged (SI) and neutral (SN) silica monomers (see Figure 4a of the main document). This was done using the utility *g_mindist* by fixing a cut-off distance of 0.97 nm and dividing the value obtained by the total number of SI or SN species in solution (i.e. 230 for SI and 770 for SN). Figure S16 shows that

during the simulation time an overwhelmingly larger number of contacts are formed between surfactant heads and anionic silica monomers, supporting the idea that SI monomers will strongly adsorb on DDA⁺ micelles while SN-head contacts are residual.

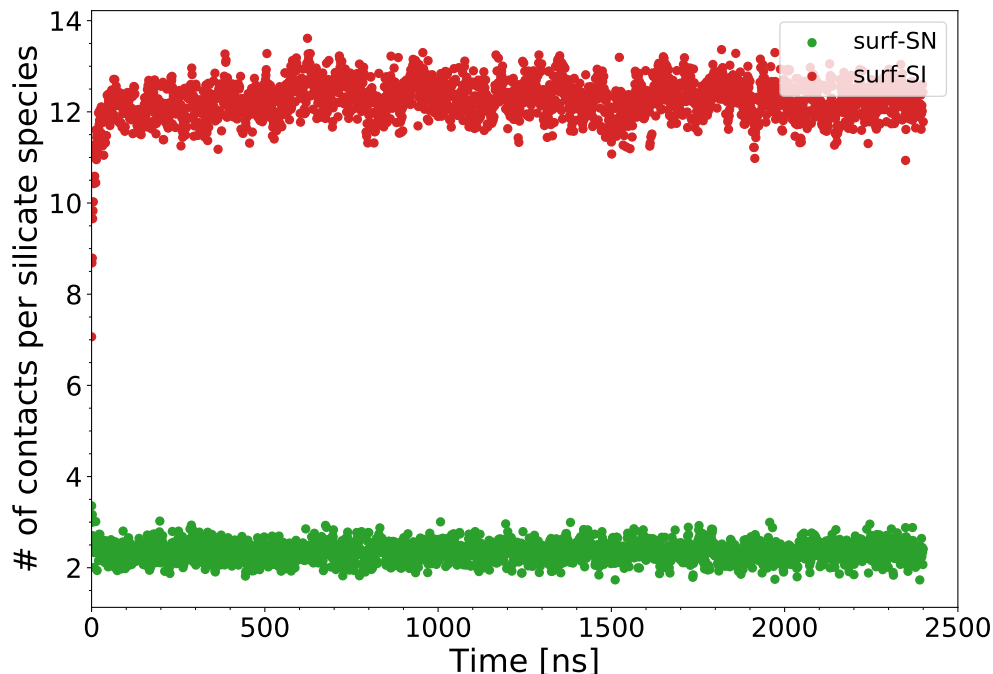


Figure S16: Number of contacts per silicate species obtained for the system containing charged surfactants and both SI and SN silica. Surfactants-SI, red and Surfactants-SN, green.

Hydrogen bond analysis To better understand the interactions occurring in the neutral system, formation of hydrogen bonds was assessed using the utility *g_hbond* based on AA simulations of silica/surfactant solutions. Indeed, hydrogen bonds are formed between neutral silica monomers and the neutral surfactant heads. However, calculation of the donor-acceptor distribution distances indicates that this interaction is quite weak compared to the other hydrogen bond interactions taking place in the system (see Figure S17).

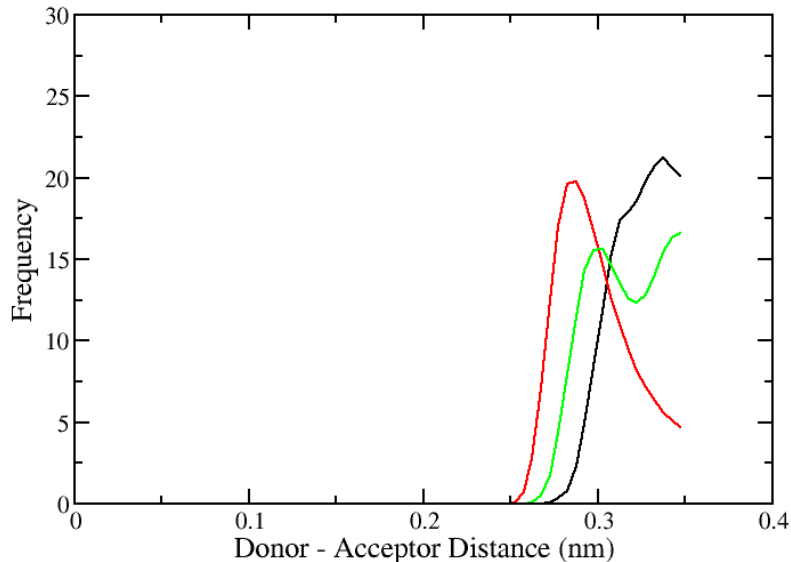


Figure S17: Distributions of donor-acceptor distances for the system containing a preformed micelle of DDA with SN monomers. Black, between surfactant heads and SN monomers; red, between surfactant heads and water; green, between SN monomers and water.

As described by Jeffrey, hydrogen bonds can be classified according to their donor-acceptor distance into “strong, mostly covalent” (between 0.22 and 0.25 nm), “moderate, mostly electrostatic” (between 0.25 and 0.32 nm) and “weak, electrostatic” (between 0.32 and 0.4 nm)²². Figure S17 shows that the donor-acceptor distance for the hydrogen bonds formed between surfactant heads and SN monomers (black line) is in the range of weak electrostatic interactions, whereas the hydrogen bonds formed by water with surfactant heads and SN monomers (red and green lines, respectively) correspond to moderate electrostatic interactions. As such, the affinity observed between SN and surfactants micelles is most likely due to hydrophobic interactions than to hydrogen bond formation in these systems.

References

- (1) Tanev, P. T.; Pinnavaia, T. J. A Neutral Templating Route to Mesoporous Molecular Sieves. **1995**, *267*, 865–867.
- (2) National Institute of Advanced Industrial Science and Technology Spectral database SDBS. 1999; <https://sdb.sdb.aist.go.jp/sdb/cgi-bin/landingpage?sdbno=2391>, [Online accessed 05-September-2018].
- (3) Berendsen, H. J. C.; Grigera, J. R.; Straatsma, T. P. The missing term in effective pair potentials. *The Journal of Physical Chemistry* **1987**, *91*, 6269–6271.
- (4) Jorgensen, W. L.; Maxwell, D. S.; Tirado-Rives, J. Development and Testing of the OPLS All-Atom Force Field on Conformational Energetics and Properties of Organic Liquids. *Journal of the American Chemical Society* **1996**, *118*, 11225–11236.
- (5) Wang, J.; Wolf, R. M.; Caldwell, J. W.; Kollman, P. A.; Case, D. A. Development and testing of a general amber force field. *Journal of Computational Chemistry* **2004**, *25*, 1157–1174.
- (6) Jorge, M.; Gomes, J. R. B.; Cordeiro, M. N. D. S.; Seaton, N. A. Molecular Dynamics Simulation of the Early Stages of the Synthesis of Periodic Mesoporous Silica. *The Journal of Physical Chemistry B* **2009**, *113*, 708–718.
- (7) Hess, B.; Bekker, H.; Berendsen, H. J. C.; Fraaije, J. G. E. M. LINCS: A linear constraint solver for molecular simulations. *Journal of Computational Chemistry* **1997**, *18*, 1463–1472.
- (8) Darden, T.; York, D.; Pedersen, L. Particle mesh Ewald: An $N \log(N)$ method for Ewald sums in large systems. *The Journal of Chemical Physics* **1993**, *98*, 10089–10092.
- (9) Darden, T.; Perera, L.; Li, L.; Pedersen, L. New tricks for modelers from the crystallog-

- raphy toolkit: the particle mesh Ewald algorithm and its use in nucleic acid simulations. *Structure* **1999**, *7*, R55–R60.
- (10) Martínez, L.; Andrade, R.; Birgin, E. G.; Martínez, J. M. PACKMOL: a package for building initial configurations for molecular dynamics simulations. *Journal of Computational Chemistry* **2009**, *30*, 2157–2164.
- (11) Malliaris, A.; Le Moigne, J.; Sturm, J.; Zana, R. Temperature dependence of the micelle aggregation number and rate of intramicellar excimer formation in aqueous surfactant solutions. *The Journal of Physical Chemistry* **1985**, *89*, 2709–2713.
- (12) Jorge, M.; Gomes, J. R. B.; Cordeiro, M. N. D. S.; Seaton, N. A. Molecular Simulation of Silica/Surfactant Self-Assembly in the Synthesis of Periodic Mesoporous Silicas. *Journal of the American Chemical Society* **2007**, *129*, 15414–15415.
- (13) Jorge, M. Molecular Dynamics Simulation of Self-Assembly of n-Decyltrimethylammonium Bromide Micelles. *Langmuir* **2008**, *24*, 5714–5725.
- (14) Nosé, S. A molecular dynamics method for simulations in the canonical ensemble. *Molecular Physics* **1984**, *52*, 255–268.
- (15) Parrinello, M.; Rahman, A. Polymorphic transitions in single crystals: A new molecular dynamics method. *Journal of Applied Physics* **1981**, *52*, 7182–7190.
- (16) Hockney, R.; Goel, S.; Eastwood, J. Quiet high-resolution computer models of a plasma. *Journal of Computational Physics* **1974**, *14*, 148–158.
- (17) Marrink, S. J.; Risselada, H. J.; Yefimov, S.; Tieleman, D. P.; de Vries, A. H. The MARTINI Force Field: Coarse Grained Model for Biomolecular Simulations. *J. Phys. Chem. B* **2007**, *111*, 7812–7824.
- (18) Pérez-Sánchez, G.; Chien, S.-C.; Gomes, J. R. B.; Cordeiro, M. N. D. S.; Auerbach, S. M.; Monson, P. A.; Jorge, M. Multiscale Model for the Templated Synthesis

of Mesoporous Silica: The Essential Role of Silica Oligomers. *Chemistry of Materials* **2016**,

- (19) Bussi, G.; Donadio, D.; Parrinello, M. Canonical sampling through velocity rescaling. *The Journal of Chemical Physics* **2007**, *126*, 014101.
- (20) Hoshen, J.; Kopelman, R. Percolation and cluster distribution. I. Cluster multiple labeling technique and critical concentration algorithm. *Physical Review B* **1976**, *14*, 3438–3445.
- (21) CAMEO Chemicals, DODECANAMINE | CAMEO Chemicals | NOAA. <https://cameochemicals.noaa.gov/chemical/21833>, [Online accessed 13-March-2017].
- (22) Jeffrey, G. *An Introduction to Hydrogen Bonding*; Topics in Physical Chemistry - Oxford University Press; Oxford University Press, 1997.